

Mono- VH Dark Matter Search Using 13 TeV Data

Xuanhong Lou, Peking University, Beijing, China

Jike Wang, DESY, Hamburg, Germany

September 18, 2015

Abstract

In search of dark matter produced in association with a W , Z or H boson we present data and Monte Carlo comparison at signal region and $Z \rightarrow ll$ control region in proton-proton collisions representing 0.0787 fb^{-1} of integrated luminosity at a center-of-mass energy of 13 TeV using data recorded with the ATLAS detector at the CERN Large Hadron Collider Run 2. The region definitions are based on fat-jet selection. A newly developed boosted V tagger's performance on 2 TeV mass Heavy Vector Triplet $HVT \rightarrow WZ \rightarrow \nu\nu qq$ signal is examined then. The signal efficiency and sensitivity for various W cuts are also given.

Contents

| | | |
|----------|---|-----------|
| 1 | Introduction | 3 |
| 2 | Framework and Dataset | 3 |
| 3 | $Z \rightarrow \ell\ell$ Control Region | 4 |
| 4 | Signal Region | 7 |
| 4.1 | Fat-jet basic selection | 7 |
| 4.2 | MPT cuts | 7 |
| 4.3 | Anti-QCD cut | 9 |
| 5 | Boosted V Tagger Performance | 9 |
| 5.1 | W mass cut performance | 12 |
| 5.2 | W tagger D_2 cut performance | 12 |
| 5.3 | Signal efficiency and sensitivity | 13 |
| 6 | Conclusion | 13 |
| 7 | Acknowledgement | 14 |

1 Introduction

Though most of the matter in the Universe is dark matter (DM), little is known of its underlying particle nature or its nongravitational interactions. We attempt to shed light on this mystery with a search for dark matter produced in association with a hadronically decaying vector boson or Higgs boson using 13 TeV proton-proton collisions at the LHC collider.

DM production at colliders is characterized by events with missing transverse energy (E_T^{miss}) caused by DM particles escaping detection and recoiling against a visible final state X . The recent mono- X studies at the LHC searches for a variety of different $E_T^{miss} + X$ signals, where X is a hadronic jet (j) [1–4], photon (γ) [5–8], or W or Z boson (V) [9–13].

With the discovery of the Higgs boson [14, 15], a new window to DM has opened. If DM is indeed associated with the scale of electroweak symmetry breaking [16, 17], Higgs-boson-related signatures in colliders provide a natural place to search for it. A recent paper [18] explored the theoretical aspects of this new LHC signature of dark matter: DM pair production in association with a Higgs boson, $H\chi\chi$, dubbed ‘mono-Higgs’, giving a detector signature of $H + E_T^{miss}$.

In this article we will give data and Monte Carlo (MC) comparison at signal region and $Z \rightarrow ll$ control region in proton-proton collisions with 0.0787 fb^{-1} of integrated luminosity at a center-of-mass energy of 13 TeV. The framework and dataset we are using will be discussed in Section 2. In Section 3 the $Z \rightarrow ll$ control plots will be presented, with signal region being discussed in Section 4. Then we examine the performance of the newly developed boosted V tagger and give the signal efficiency and sensitivity for various W cuts in Section 5. Section 6 gives a brief conclusion of our study.

2 Framework and Dataset

The framework we use for data analysis is hsg5framework¹, especially the CxAOD-Maker_VHbb and CxAODReader_monoVH packages.

For $Z \rightarrow ll$ control region analysis, we use HSG5 HIGG2D4 CxAOD 00-12-01 as input. Three missing p_t slices² are produced by self using official DxAOD release³.

The data and MC samples for signal region studies are from HSG5 HIGG5D1 CxAOD 00-12-01. Twenty-nine p_t slices⁴ are missing and produced by self using official DxAOD

¹svn+ssh://svn.cern.ch/repos/atlasoff/PhysicsAnalysis/HiggsPhys/Run2/Hbb/CxAODFramework/

²ZeeB 70-140GeV, ZmumuB 140-280GeV, ZmumuL 140-280GeV

³mc15_13TeV.*.Sherpa_CT10.*.merge.DAOD_HIGG2D4.*r6264_p2375

⁴WenuB 140-280GeV, WenuC 0-70GeV, WenuC 280-500GeV, WmumuB 0-70GeV, WmumuB 280-500GeV, WmumuC 0-70GeV, WtaunuB 0-70GeV, WtaunuB 140-280GeV, WtaunuB 500-700GeV, WtaunuB 700-1000GeV, WtaunuC 70-140GeV, WtaunuL 0-70GeV, WtaunuL 70-140GeV, WtaunuL 140-280GeV, WtaunuL 280-500GeV, ZeeB 70-140GeV, ZeeC 140-280GeV, ZmumuB 0-70GeV, ZmumuL 140-280GeV, ZnnuL 500-700GeV, ZtautauB 70-140GeV, ZtautauB 140-280GeV, ZtautauB 500-700GeV, ZtautauC 70-140GeV, ZtautauC 140-280GeV, ZtautauC 280-500GeV, ZtautauC 700-1000GeV, ZtautauL 0-70GeV, ZtautauL 140-280GeV

release⁵.

The boosted V tagger we apply to signal region selection is developed by ATLAS jet substructure group⁶. The configuration file we use is 20150809 version⁷.

3 $Z \rightarrow \ell\ell$ Control Region

In order to provide regions in which the yield of background events can be estimated, certain event-level cuts are applied to create control regions (CR).

All input events for our $Z \rightarrow \ell\ell$ CR studies have already passed through a loose lepton pre-selection at CxAOD level, which requires for 2 leptons with transverse momentum over 7 GeV. This control region is defined as events which contain exactly 2 tight electrons or muons with tight isolation, at least 1 AntiKt10LCTopoTrimmedPtFrac5-SmallR20Jet with $p_t > 150$ GeV and $|\eta| < 1.2$. The combined $mass_Z$ of 2 leptons must be between 75 to 105 GeV. Additional selection includes 0 b-tagged AntiKt4EMTopoJet. Figure 1 and Figure 2 shows the 0 b-tagged electron/muon control plots for $Z \rightarrow \ell\ell$ CR, with overall good data and MC agreement. For 1 b-tagged and 2 b-tagged Figure 3, Figure 4, Figure 5 and Figure 6 the statistical fluctuation begins to play a more dominant part.

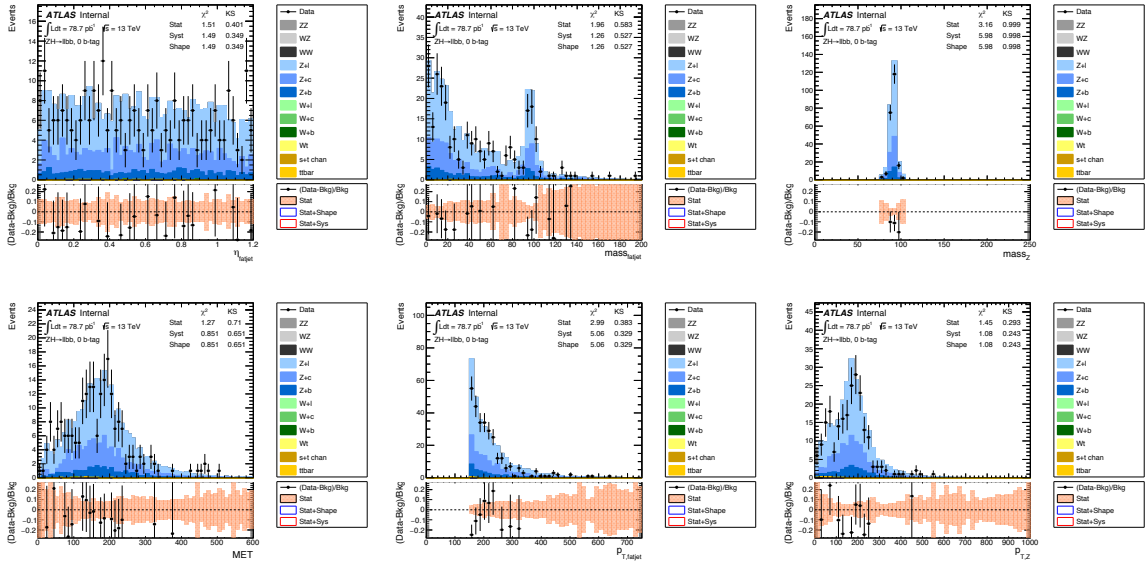


Figure 1: Electron control plots, 0 b-tagged

⁵mc15_13TeV.*.Sherpa_CT10.*.merge.DAOD_HIGG5D1.*r6264_p2375

⁶svn+ssh://svn.cern.ch/repos/atlasoff/Reconstruction/Jet/JetSubStructureUtils/tags/JetSubStructureUtils-00-02-12/

⁷config_13TeV_Wtagging_MC15_Prerecommendations_20150809.dat

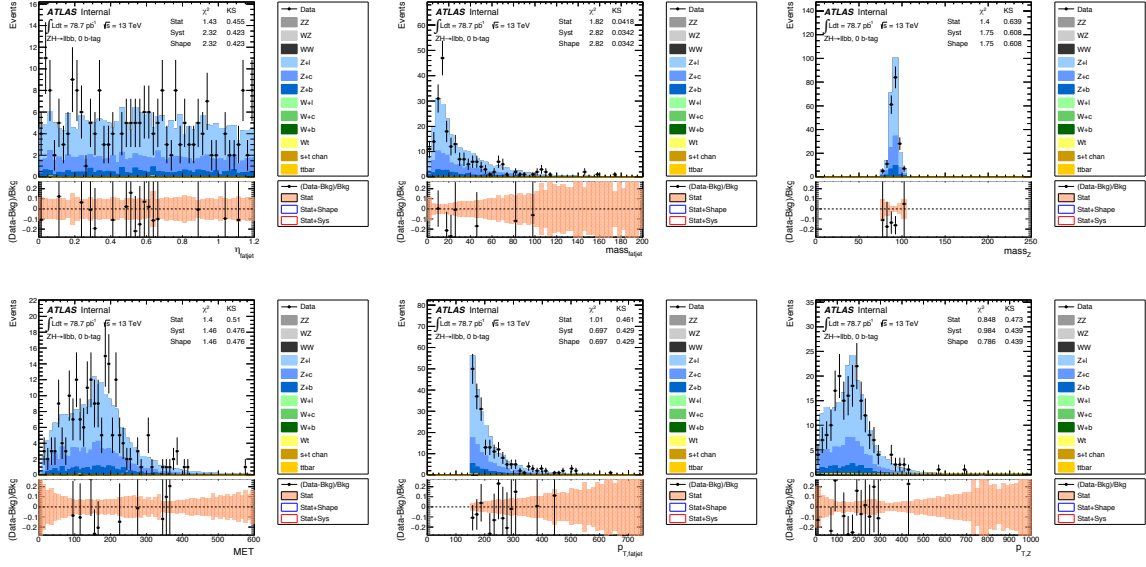


Figure 2: Muon control plots, 0 b-tagged

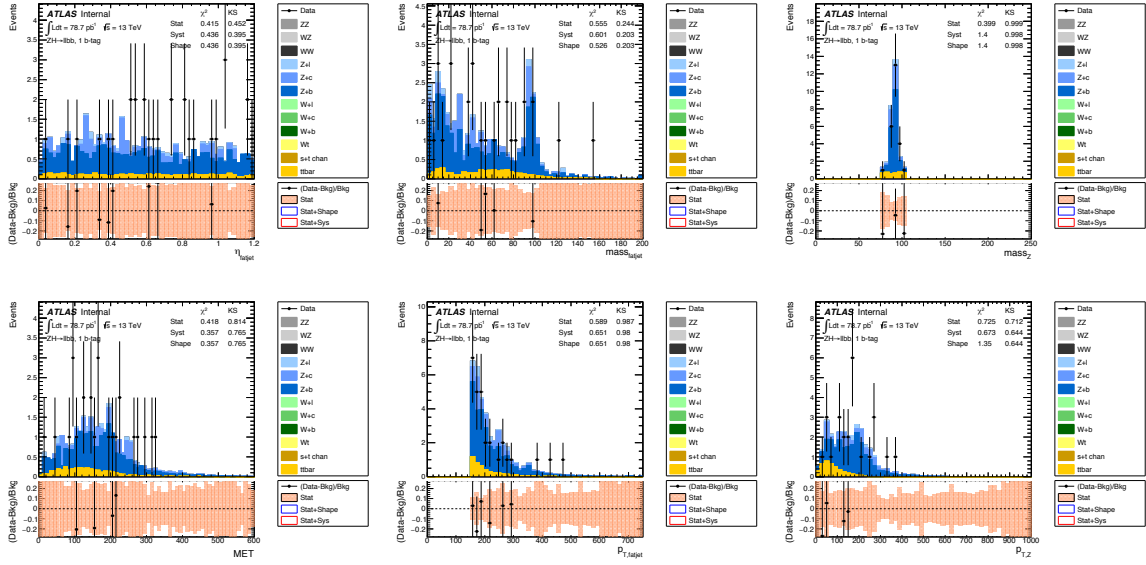
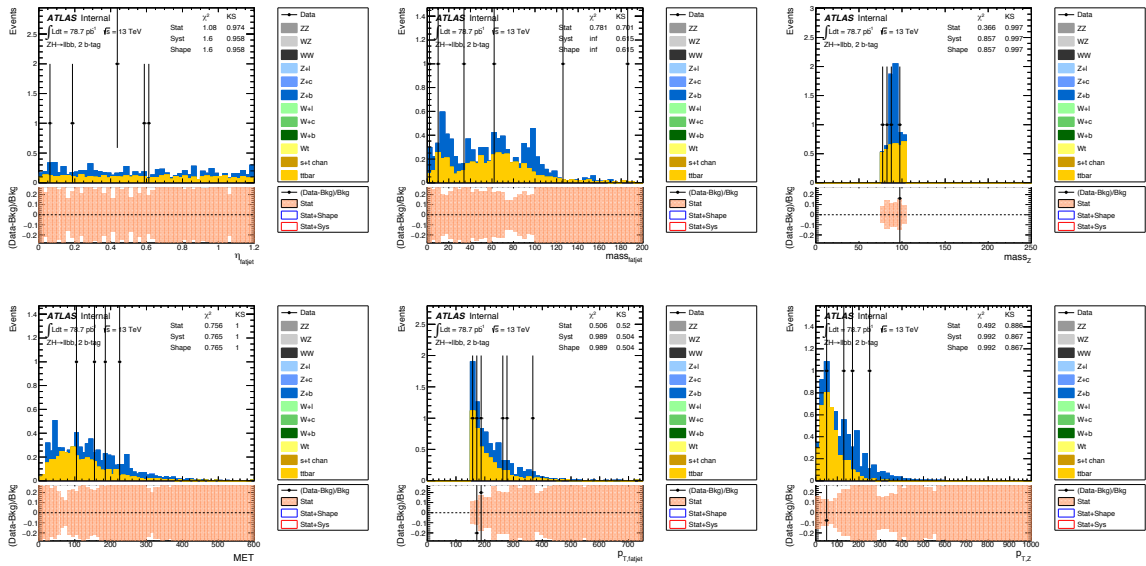
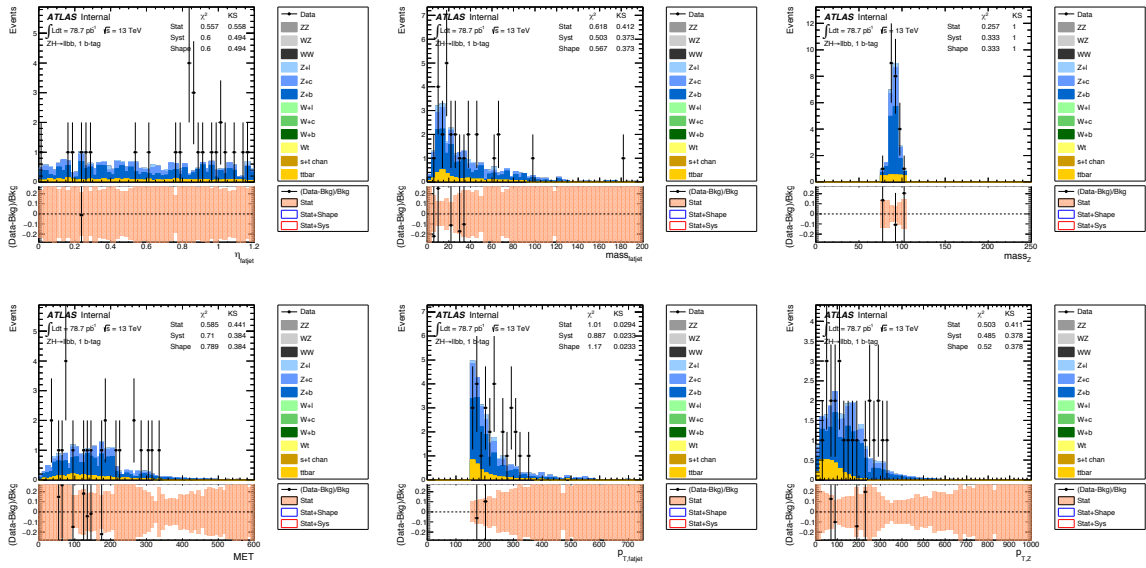


Figure 3: Electron control plots, 1 b-tagged



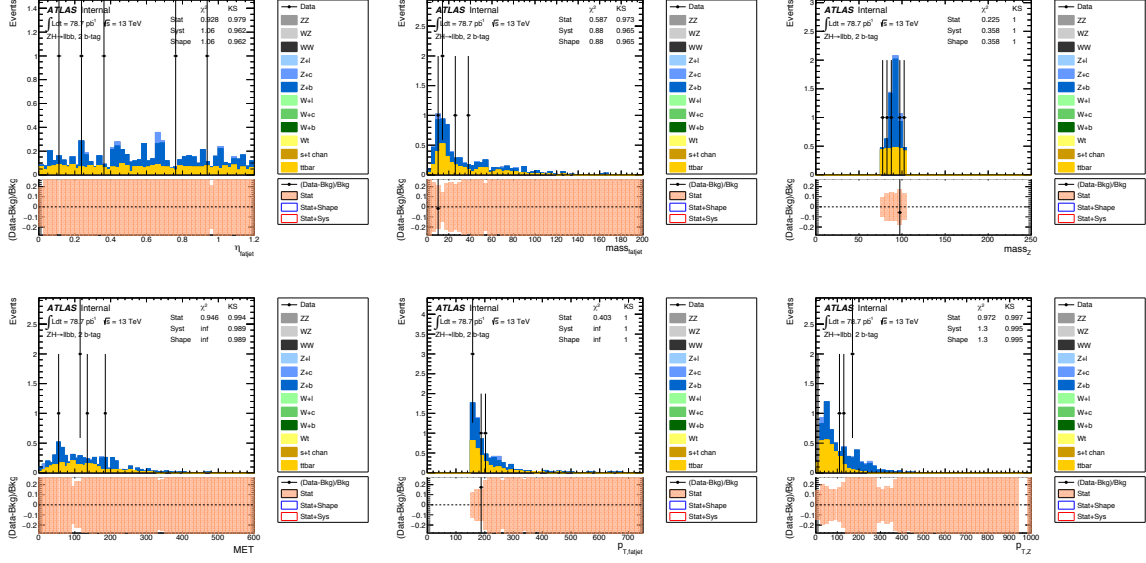


Figure 6: Muon control plots, 2 b-tagged

4 Signal Region

4.1 Fat-jet basic selection

The signal region (SR) selection criteria are designed to maximize the acceptance of the expected signal topology while reducing other backgrounds' contributions to a minimum. Here we implement fat-jet filter at SR studies for the first time and use 2 TeV mass Heavy Vector Triplet $HVT \rightarrow WZ \rightarrow \nu\nu qq$ samples as DM signal, with $Z \rightarrow \nu\nu$ process mimicking DM pair production.

Input events have already passed through a loose lepton pre-selection at CxAOD level, which requires for zero lepton with transverse momentum over 7 GeV. The basic SR selection is defined as events which contain at least 1 AntiKt10LCTopoTrimmedPtFrac5-SmallR20Jet with $p_t > 250$ GeV and $|\eta| < 2.0$. An $E_T^{miss} > 160$ GeV cut is applied separately.

Figure 7 shows data and MC comparison after basic selection. The data is 4 times larger than background on average.

4.2 MPT cuts

The huge disagreement between MC and data is due to non-collision background. When doing simulation, each MC event can be categorized into one certain decay mode: ttbar, multijet, gammajet, etc. But for real data recorded by detector, there can be some events which don't belong to any of these decay modes. In order to veto these background events, the track-based missing transverse momentum vector (MPT) cuts are introduced then. MPT is calculated as the negative vector sum of transverse momenta

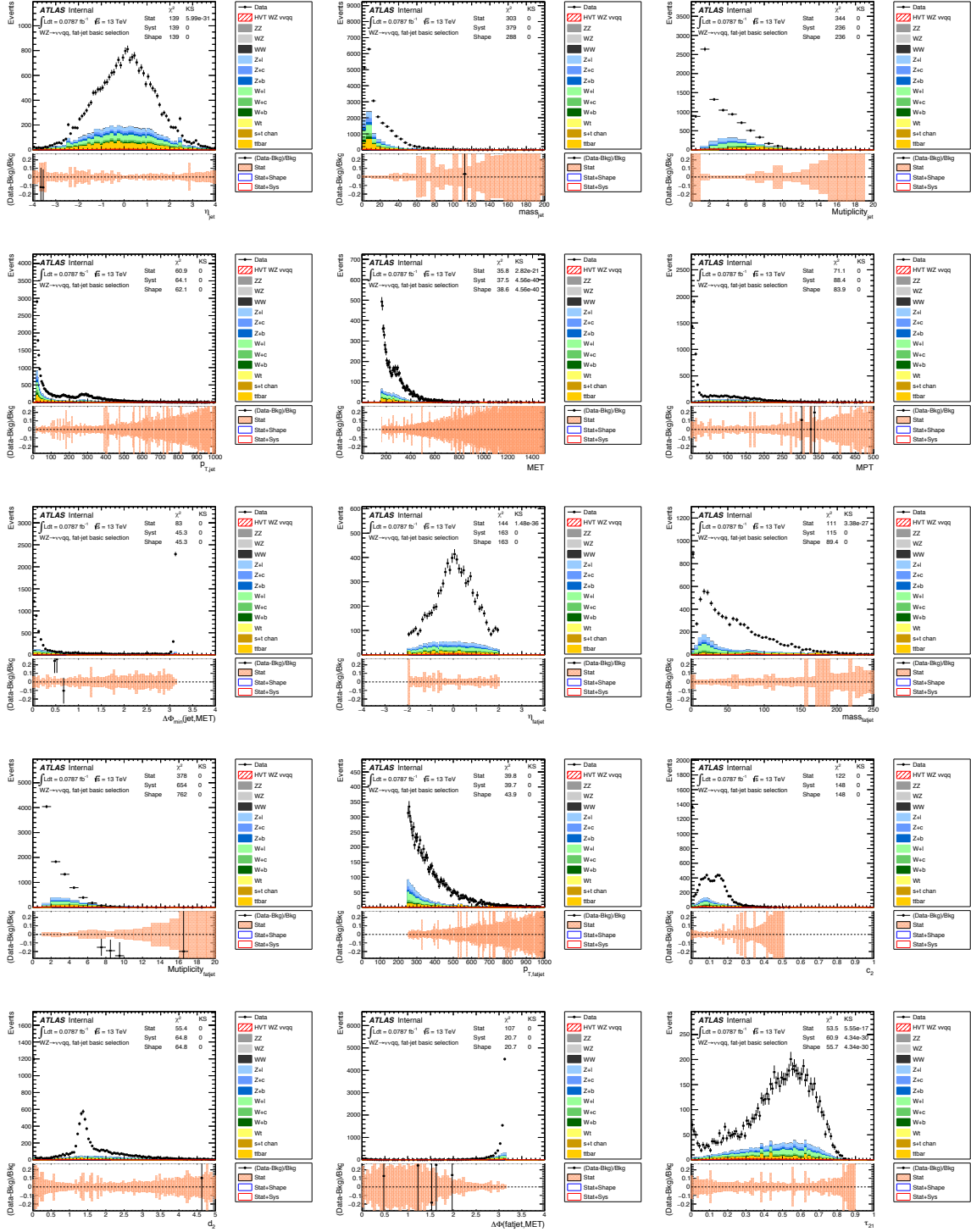


Figure 7: Fat-jet basic selection

of reconstructed tracks associated with the primary vertex and within $|\eta| < 2.5$, while non-collision background has no track information. From the MPT distribution plot shown in Figure 7, we can clearly see that the MC-data difference, which indicates non-collision events, dominates the low MPT area.

Two additional cuts ask events to have $p_T^{miss} > 30$ GeV and $\Delta\phi(p_T^{miss}, E_T^{miss}) < \pi/2$. In Figure 8 we can see much improvement on data and MC agreement after MPT cuts applied: the data is only twice as large as MC background now.

4.3 Anti-QCD cut

Next step is to remove QCD backgrounds which we are not interested in. An easy way is making use of the $\min\Delta\phi(jets, E_T^{miss})$ variable. For QCD events, the detector can possibly miss some jet constituents and result in energy difference between truth jet and reconstructed jet, which will be considered as E_T^{miss} when rebuilding. If the E_T^{miss} of certain event mainly comes from this mechanism, the minimum angle between E_T^{miss} and jets would be rather small, because the calculated missing transverse energy is actually part of its nearest jet.

However for DM signal events, the E_T^{miss} , which represents invisible DM particles, should be back to the recoiling jet according to conservation laws. Thus its $\min\Delta\phi(jets, E_T^{miss})$ should be close to π .

Here we choose a $\min\Delta\phi(jets, E_T^{miss}) > 1.5$ cut for our SR selection. The result is shown in Figure 9.

5 Boosted V Tagger Performance

Based on SR selection, we further apply the newly developed boosted V tagger to our study. The W tagger configuration is used to optimize our $HVT \rightarrow WZ \rightarrow \nu\nu qq$ signal. Various W cut for comparison are listed below:

- Simple W mass window cut ($60 \text{ GeV} < mass_W < 105 \text{ GeV}$)
- W tagger cuts, medium/tight working point⁸
 - return 1, only pass D_2 selection
 - return 2, only pass mass selection
 - return 3, pass mass and D_2 selection
 - return 1 or 3, pass D_2 selection
 - return 2 or 3, pass mass selection

⁸return (passMass<<1)|(passSub<<0)

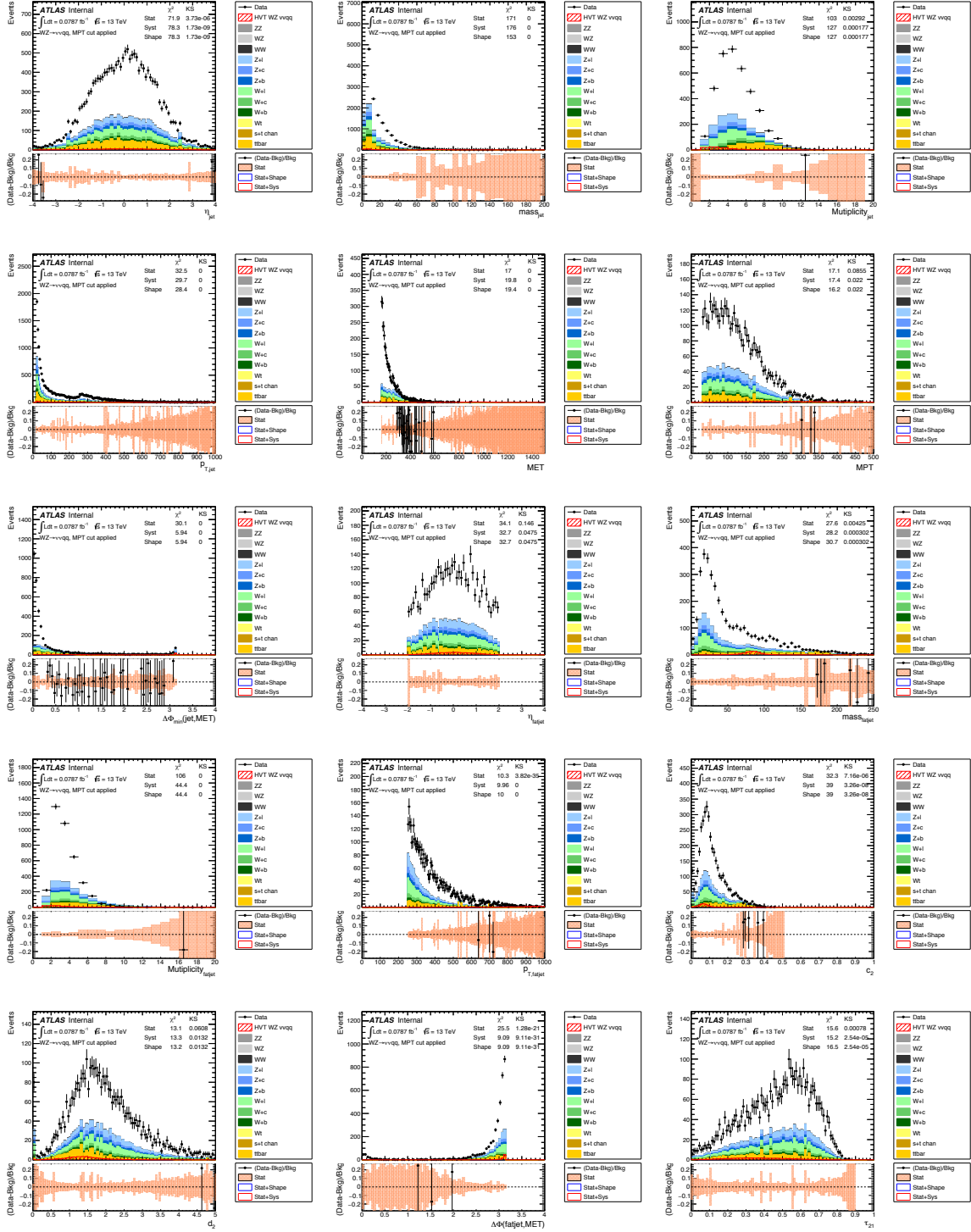


Figure 8: Signal region selection, MPT cuts applied

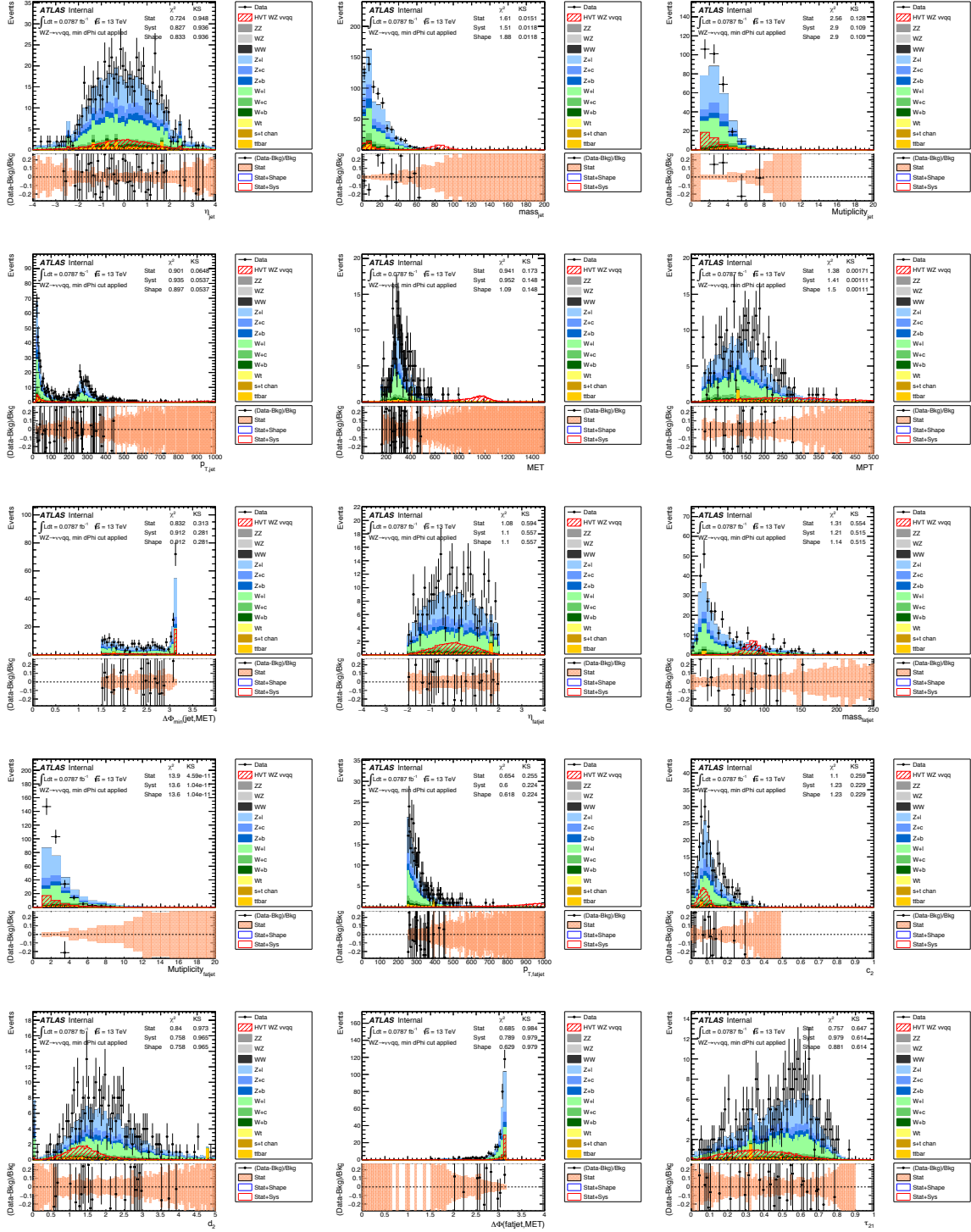


Figure 9: Signal region selection, anti-QCD cut applied

5.1 W mass cut performance

As shown in Figure 10, the $p_{T,fatjet}$ dependent W tagger mass cuts present better background rejection than simple W mass window cut. The medium/tight working points actually share same set of mass selection parameter.

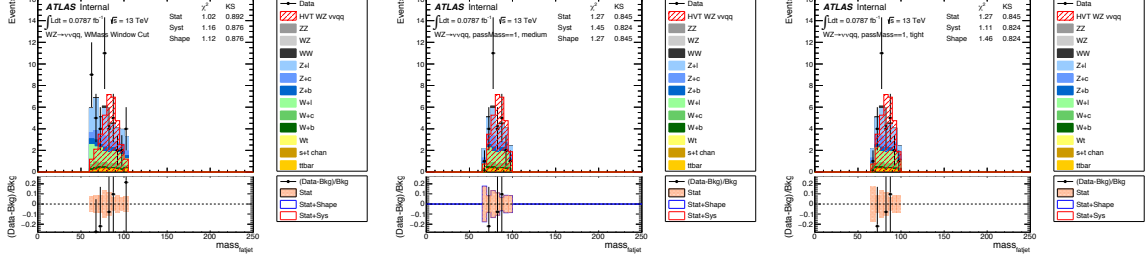


Figure 10: $mass_{fatjet}$ distribution after different W cuts. left: simple W mass window cut; middle: W tagger mass cut, medium working point; right: W tagger mass cut, tight working point

Figure 11 shows the D_2 distribution plots after different W cuts. W mass cuts have no separation power on this jet substructure variable. Specialized D_2 selection technique needs to be introduced.

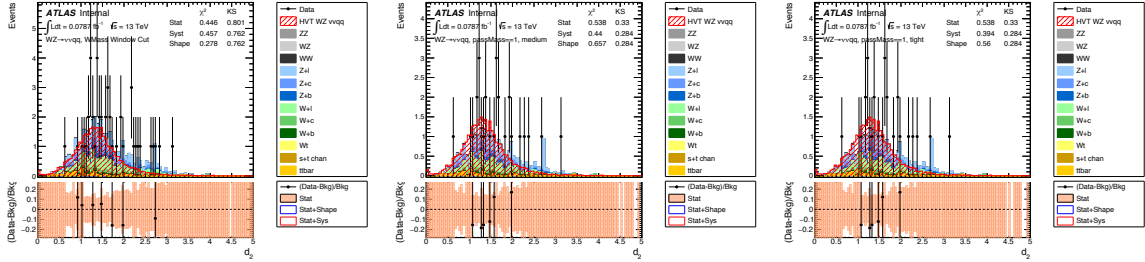


Figure 11: D_2 distribution after different W cuts. left: simple W mass window cut; middle: W tagger mass cut, medium working point; right: W tagger mass cut, tight working point

5.2 W tagger D_2 cut performance

2D view, Figure 12 points out the mechanism of jet substructure selection in W tagger. The tagger calculates an expected D_2 value using a quartic function of $p_{T,fatjet}$. Then it vetoes all events with D_2 above this value. Grey curve in the plots indicates the D_2 cut at medium working point; the darker one is for tight working point.

It is obvious that the current jet substructure selection in boosted W tagger is not optimal for our HVT $WZ \rightarrow \nu\nu qq$ signal⁹.

⁹this tagging tool is designed based on $HVT \rightarrow WZ \rightarrow qq qq$ signal

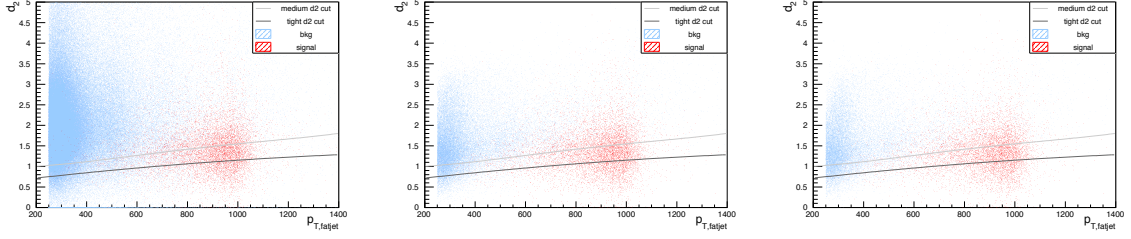


Figure 12: D_2 versus $p_{T,fatjet}$ scattering plots. left: no W cut applied; middle: simple W mass window cut; right: W tagger mass cut, medium/tight working point

5.3 Signal efficiency and sensitivity

The signal efficiency and sensitivity for various W cuts are listed in Table 1. Note that an additional $E_T^{miss} > 600$ GeV cut is applied in order to optimize signal sensitivity. Here efficiency is defined as $n_{signal}/n_{signal,nocut}$, where $n_{signal,nocut} = 37.58$, and sensitivity is defined as $n_{signal}/\sqrt{n_{background}}$. All signal event numbers appearing on the table and used for calculation have been scaled down to 1 %.

| | Signal | Background | Efficiency | Sensitivity |
|-------------------------------|--------|------------|------------|-------------|
| Simple W mass window cut | 0.3300 | 0.9520 | 87.81% | 0.3382 |
| W tagger medium, return 1 | 0.0344 | 1.3109 | 9.15% | 0.0300 |
| W tagger medium, return 2 | 0.1066 | 0.5823 | 28.37% | 0.1397 |
| W tagger medium, return 3 | 0.1819 | 0.0801 | 48.40% | 0.6427 |
| W tagger medium, pass D_2 | 0.2163 | 1.3910 | 57.56% | 0.1834 |
| W tagger medium, pass mass | 0.2885 | 0.6624 | 76.77% | 0.3545 |
| W tagger tight, return 1 | 0.0131 | 0.8425 | 3.49% | 0.0143 |
| W tagger tight, return 2 | 0.2028 | 0.6436 | 53.96% | 0.2528 |
| W tagger tight, return 3 | 0.0857 | 0.0188 | 22.80% | 0.6250 |
| W tagger tight, pass D_2 | 0.0988 | 0.8613 | 26.29% | 0.1065 |
| W tagger tight, pass mass | 0.2885 | 0.6624 | 76.77% | 0.3545 |

Table 1: Signal efficiency and sensitivity (after $E_T^{miss} > 600$ GeV cut)

6 Conclusion

In this article, we present detailed study at $Z \rightarrow ll$ control region as well as signal region in search of dark matter using LHC Run 2 result.

The new 13 TeV data behaves in good agreement with MC15 simulation samples at $Z \rightarrow ll$ CR after going through the 2 lepton filter, the fat-jet selection and a reconstructed Z mass window cut. Additionally, b-jet control plots are provided for both electron and muon region. These results will help us better understand $Z \rightarrow ll$ decay

mode and improve the precision of background estimation in our future work.

For signal region studies, we apply fat-jet to event selection for the first time and observe very good agreement between data and MC. Base on fat-jet basic selection, MPT related cuts are used to reject non-collision events, while a $\min\Delta\phi(jets, E_T^{miss})$ cut vetoes QCD background.

Further, a W tagging tool is tested on top of our SR selection. Results suggest that the $p_{T,fatjet}$ dependent mass cut in tagger gives better background rejection when comparing to simple W mass window cut. On the other hand, current D_2 versus $p_{T,fatjet}$ parameterizations are not the most optimal ones and can be further improved according to our studies.

Finally we calculated the signal efficiency and sensitivity for various W cuts, with W tagger return value 3 at medium/tight working point giving best sensitivity. Considering the low signal efficiency at tight working point (around 23%), medium configuration keeps good balance on efficiency and sensitivity.

7 Acknowledgement

The completion of this work will not be possible without the kind and patient help from my supervisor Jike. I learned so much from him, from basic techniques for data analysis to enlightening life experiences about academic career.

I also need to express my gratitude to all the DESY ATLAS faculty as well as other organisers of this summer program.

Special thanks to our mono-WZH hadronic group and jet substructure group in ATLAS, thanks for all your valuable comments on my research.

References

- [1] ATLAS Collaboration, G. Aad et al., *Search for new phenomena with the monojet and missing transverse momentum signature using the ATLAS detector in $\sqrt{s} = 7$ TeV proton-proton collisions.*
- [2] CMS Collaboration, S. Chatrchyan et al., *Search for dark matter and large extra dimensions in monojet events in pp collisions at $\sqrt{s} = 7$ TeV.*
- [3] ATLAS Collaboration, G. Aad et al., *Search for new phenomena in final states with an energetic jet and large missing transverse momentum in pp collisions at $\sqrt{s} = 8$ TeV with the ATLAS detector.*
- [4] CMS Collaboration, S. Chatrchyan et al., *Search for dark matter, extra dimensions, and unparticles in monojet events in proton-proton collisions at $\sqrt{s} = 8$ TeV.*
- [5] ATLAS Collaboration, G. Aad et al., *Search for dark matter candidates and large extra dimensions in events with a photon and missing transverse momentum in pp collision data at $\sqrt{s} = 7$ TeV with the ATLAS detector.*
- [6] CMS Collaboration, S. Chatrchyan et al., *Search for Dark Matter and Large Extra Dimensions in pp Collisions Yielding a Photon and Missing Transverse Energy.*
- [7] ATLAS Collaboration, G. Aad et al., *Search for new phenomena in events with a photon and missing transverse momentum in pp collisions at $\sqrt{s} = 8$ TeV with the ATLAS detector.*
- [8] CMS Collaboration, S. Chatrchyan et al., *Search for new phenomena in monophoton final states in proton-proton collisions at $\sqrt{s} = 8$ TeV.*
- [9] L. M. Carpenter, A. Nelson, C. Shimmin, T. M. Tait, and D. Whiteson, *Collider searches for dark matter in events with a Z boson and missing energy.*
- [10] ATLAS Collaboration, G. Aad et al., *Search for dark matter in events with a hadronically decaying W or Z boson and missing transverse momentum in pp collisions at $\sqrt{s} = 8$ TeV with the ATLAS detector.*
- [11] ATLAS Collaboration, G. Aad et al., *Search for dark matter in events with a Z boson and missing transverse momentum in pp collisions at $\sqrt{s} = 8$ TeV with the ATLAS detector.*
- [12] ATLAS Collaboration, G. Aad et al., *Search for new particles in events with one lepton and missing transverse momentum in pp collisions at $\sqrt{s} = 8$ TeV with the ATLAS detector.*
- [13] CMS Collaboration, S. Chatrchyan et al., *Search for physics beyond the standard model in final states with a lepton and missing transverse energy in proton-proton collisions at $\sqrt{s} = 8$ TeV.*

- [14] ATLAS Collaboration Collaboration, G. Aad et al., *Observation of a new particle in the search for the Standard Model Higgs boson with the ATLAS detector at the LHC*.
- [15] CMS Collaboration Collaboration, S. Chatrchyan et al., *Observation of a new boson at a mass of 125 GeV with the CMS experiment at the LHC*.
- [16] G. Jungman, M. Kamionkowski, and K. Griest, *Supersymmetric dark matter*.
- [17] G. Bertone, D. Hooper, and J. Silk, *Particle dark matter: Evidence, candidates and constraints*.
- [18] L. Carpenter, A. DiFranzo, M. Mulhearn, C. Shimmin, S. Tulin, et al., *Mono-Higgs: a new collider probe of dark matter*.